Gamma-Neutron Cross Sections

H. E. JOHNS, L. KATZ, R. A. DOUGLAS, AND R. N. H. HASLAM
Betatron Group, University of Saskatchewan, Saskatoon, Saskatchewan, Canada
(Received July 17, 1950)

A method is outlined for determining the total number of photons at each energy for a given irradiation from a betatron, assuming the bremsstrahlung photon distribution to be represented by an equation of Schiff and the response of an r-meter to be proportional to the absorption cross section for photons in the wall material.

The resulting activities produced by gamma-neutron reactions in Cu^{63}, Cu^{65}, Sb^{121}, Sb^{123}, and Ta^{181} have been measured as functions of the maximum photon energy of the betatron. In each case the activity was normalized to saturation per gram for 100 roentgens of radiation.

A method is also outlined whereby these activation curves may be analyzed to give the photo-neutron cross section as a function of energy. The cross section for Cu^{63} obtained by this method has its maximum at 17.5 Mev with a resonance half-width of 6 Mev and an integrated area of 0.7 Mev—barn. Maxima for the other nuclides are at somewhat lower energies and have essentially the same half-width.

I. INTRODUCTION

PHOTO-NEUTRON disintegrations were produced by x-rays from a betatron operating with peak energies from 9 to 26 Mev. Dosage rates up to 160 r.p.m. at the samples were used. The maximum energy of the betatron was stabilized within 0.1 Mev by an integrator-expander developed by Katz *et al.*[1] Calibration was based on the threshold[2] of $Cu^{63}(\gamma, n)Cu^{62}$ at 10.9 Mev, and $C^{12}(\gamma, n)C^{11}$ at 18.7 Mev.

The energy distribution in the forward direction of the betatron beam is given by a theoretical equation of Schiff,[3,4] which is plotted on Fig. 1 for maximum photon energies of 4.5, 7.5, 11.5, 15.5, 19.5, and 24.5 Mev. This distribution is in essential agreement with the theoretical work of Heitler[5] and of Rossi and Greisen.[6]

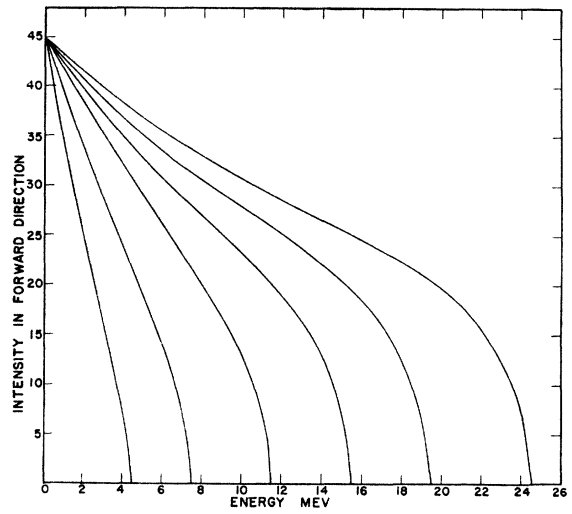

FIG. 1. Relative intensity of the bremsstrahlung in the forward direction as given by Eq. (1).

Koch and Carter[7,8] have obtained an experimental energy distribution by measuring the radius of curvature of positron and negatron tracks in a cloud chamber. Their results compare reasonably well with the Schiff distribution.

Experimental results are given for (γ, n) reactions in the following parent isotopes: Cu^{63}, Cu^{65}, Sb^{121}, Sb^{123}, and Ta^{181}. Satisfactory agreement with the work of McElhinney *et al.*[2] is obtained for Cu^{63}, approximate agreement for Ta^{181}, and exact agreement with the recent work of Almy and Diven.[9] The results differ rather widely from the work of Baldwin and Klaiber.[10] Our results indicate a broader "resonance width" than that postulated by Goldhaber and Teller,[11] though not in disagreement with the theoretical work of Levinger and Bethe.[12]

II. THEORETICAL CALCULATIONS

The intensity in the forward direction, according to Schiff[4] is proportional to

$$\Gamma = 8[2(1-z)(\ln\alpha - 1) + z^2(\ln\alpha - \tfrac{1}{2})], \qquad (1)$$

where

$$\alpha^2 = \alpha_1^2\alpha_2^2/(\alpha_1^2+\alpha_2^2),$$
$$\alpha_1 = 2E_0(1-z)/\mu z,$$

and

$$\alpha_2 = 191/Z^{\frac{1}{3}}.$$

Here μ is the rest energy of the electron, k is the energy of the photon, $z = k/E_0$, E_0 is the total energy of the electron, and Z is the atomic number of the target material.

[1] Katz, McNamara, Forsyth, Haslam, and Johns, Can. J. Research **28**, 113 (1950).
[2] McElhinney, Hanson, Becker, Duffield, and Diven, Phys. Rev. **75**, 542 (1949).
[3] I. Schiff, Phys. Rev. **70**, 87 (1946).
[4] G. D. Adams, Phys. Rev. **74**, 1707 (1948).
[5] W. Heitler, *The Quantum Theory of Radiation* (The Clarendon Press, Oxford, 1936).
[6] B. Rossi and K. Greisen, Rev. Mod. Phys. **13**, 240 (1941).
[7] H. W. Koch and R. E. Carter, Phys. Rev. **75**, 1950 (1949).
[8] H. W. Koch and R. E. Carter, Phys. Rev. **77**, 165 (1950).
[9] B. C. Diven, G. M. Almy, Phys. Rev. **80**, 407 (1950).
[10] G. C. Baldwin and G. S. Klaiber, Phys. Rev. **73**, 1156 (1948).
[11] M. Goldhaber and E. Teller, Phys. Rev. **74**, 1046 (1948).
[12] J. S. Levinger and H. A. Bethe, Phys. Rev. **78**, 115 (1950).

TABLE I. Thickness and chemical composition of the absorbers in the photon beam.

		Thickness g/cm²	Chemical composition H	C	O	Al	Si	K
Donut		2.53	···	···	0.48	0.14	0.28	0.10
Monitor	Bakelite	0.625	0.07	0.56	0.37	···	···	···
	Aluminum	0.132	···	···	···	1.00	···	···
Lucite		4.13	0.08	0.60	0.32	···	···	···

Figure 2 shows the arrangement of the experimental apparatus. The wall of the donut, the monitor, and the wall of the Lucite block affect the spectral distribution because the absorption coefficients depend upon the energy and because secondary radiation is produced. However, the probability that the secondary radiation has an energy greater than the threshold for a nuclear reaction is very small, and therefore it does not contribute to the observed activity. Unfortunately, this radiation may be recorded by the Victoreen r-meter, which is used to monitor the dose given to the samples. In general, only a small fraction of these secondary photons are emitted exactly in the forward direction, so that an r-meter subtending a small solid angle at the absorber will not be affected appreciably. This condition, known as "good geometry," is satisfied for both the donut and the monitor; but not for the Lucite block. Figure 3 shows the effect of these factors upon the theoretical distribution as follows:

A. Theoretical Schiff distribution for a maximum photon energy of 24.5 Mev.

B. Curve A modified by the absorption of the donut and monitor using total absorption coefficients.

C. Curve B modified by the absorption of the Lucite block using real absorption coefficients. This distribution assumes that all the secondary scattered radiation from the Lucite block is detected.

D. Curve B modified by the absorption of the Lucite block using total absorption coefficients. This curve neglects the secondary radiation and gives the distribution which produces photodisintegration. The Victoreen will respond to some distribution lying between C and D, but C is probably a closer approximation and so has been used in all subsequent calculations. In any case, the percentage difference is small. Table I gives the data for these calculations.

The energy flux in ergs/cm² is obtained by measuring the ionization which the beam of photons produces in the cavity of a material with known absorption coefficients. The ionization J_v in a cavity filled with air and completely surrounded by this material is given by the

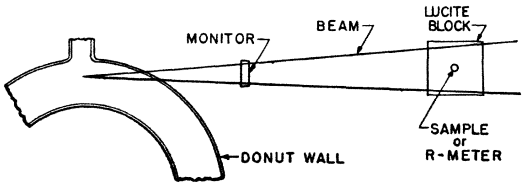

FIG. 2. Sketch of the apparatus showing the relative positions of the donut, monitor, and sample.

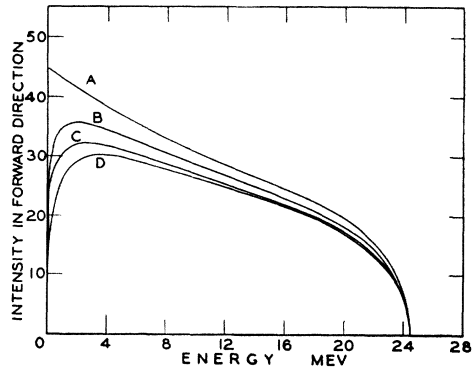

FIG. 3. Effect of absorption on the photon distribution: *A*. Theoretical Schiff distribution for a maximum photon energy of 24.5 Mev. *B*. Curve A modified by the absorption of the donut and monitor using total absorption coefficients. *C*. Curve B modified by the absorption of the Lucite block using real absorption coefficients. *D*. Curve B modified by the absorption of the Lucite block using total absorption coefficients.

well-known formula of Gray:[13]

$$J_v=(E_v/\rho W)\ \text{e.s.u./cm}^3, \qquad (2)$$

where E_v is the energy truly absorbed per unit volume of wall in ergs/cm³, ρ is the ratio of the loss of energy suffered by a beta-particle in traversing 1 cm of the wall compared to the loss in 1 cm of air, and W is the average energy per e.s.u. required to produce a pair of ions.

This equation is correct only if the wall thickness is sufficient to produce equilibrium between the electromagnetic radiation and the corpuscular radiation arising from its absorption. The actual wall thickness is of the

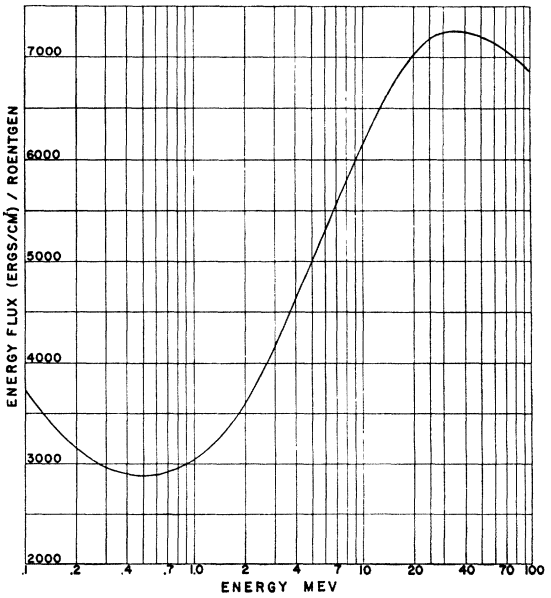

FIG. 4. Energy flux required to produce one "roentgen" measured in an air cavity in Lucite, as a function of the energy of the radiation.

[13] L. H. Gray, Proc. Roy. Soc. **A156**, 578 (1936).

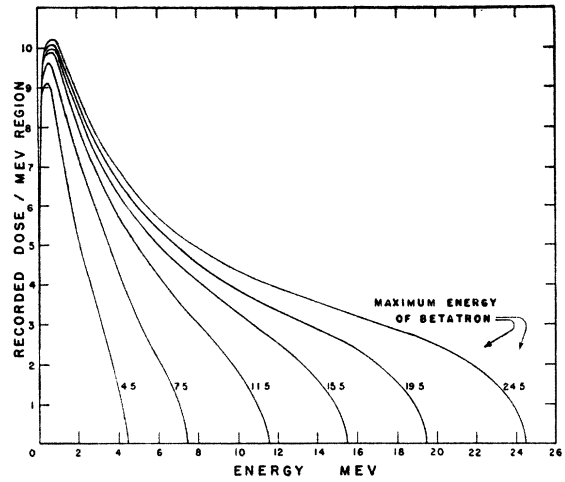

FIG. 5. Relative roentgens recorded on the basis of the respective curves of Fig. 1. This is obtained by dividing each of the curves represented by curve C of Fig. 3, by the curve of Fig. 4.

order of the mean range of the electrons. For 25 Mev, betatron radiation this is about 4 cm of Lucite. Equation (2) can be put in slightly different form since

$$E_v = E\cdot({}_e\mu_a)_w\cdot n_w \quad \text{and} \quad \rho = n_w {}_eS_w/n_a {}_eS_a,$$

where E is the energy flux of the incident beam in ergs/cm², $({}_e\mu_a)_w$ is the real absorption coefficient of the wall in cm²/electron, n_w is the number of electrons per cm³ of the wall, n_a is the number of electrons per cm³ of air, ${}_eS_w$ is the ratio of the stopping power per electron of the wall relative to air, and ${}_eS_a$ is the ratio of the stopping power per electron of air compared to air. (This is unity, but is included to maintain symmetry.) Therefore,

$$J_v = \frac{E\cdot({}_e\mu_a)_w\cdot n_w}{W\cdot(n_w {}_eS_w/n_a {}_eS_a)} = \frac{E\cdot({}_e\mu_a)_w\cdot n_a}{W({}_eS_w/{}_eS_a)}. \tag{3}$$

The number of electrons per gram of air is given by $n = n_a/0.001293$. Since it requires 32.5 ev to produce an ion pair, Eq. (3) can be written as

$$J_v = \frac{E\cdot({}_e\mu_a)_w\cdot n}{83({}_eS_w/{}_eS_a)}. \tag{4}$$

Figure 4 is a plot of E/J_v, using $n = 3.007\times10^{23}$ electron/g and[13]

$${}_eS_w/{}_eS_a = 1.02 \quad \text{(Lucite)}.$$

In this paper the dose as measured in a Lucite block will be referred to as the dose in "roentgens." This does not correspond exactly to the formal definition of the roentgen because the ionization is produced in the walls surrounding the cavity, which do not have the same absorption coefficients as air. In actual fact, the dose in true roentgens would be 2 to 15 percent greater, depending on the photon energy, for the same exposure if a true air wall material were used.

Figure 4 thus gives the energy flux at each energy which is required to record a dose of one "roentgen" for an r-meter placed in a Lucite block. Above 40 Mev the response curve begins to drop, owing to the increase in the real absorption coefficient of Lucite through pair production. The minimum at 0.5 Mev corresponds to the peak in the real Compton absorption at this energy. Below 0.1 Mev the curve rises slightly and then falls to zero as zero photon energy is approached, owing to the very large photoelectric absorption at low energies.

To normalize the distribution curves, the series of curves represented by curve C of Fig. 3 is divided by the response curve of the r-meter (Fig. 4), giving the curves of Fig. 5.

The area under each one of the curves of Fig. 5 is proportional to the number of recorded "r." Normalizing each of these to 100 r will determine the actual ordinates of Fig. 1 and Fig. 3. Using this normalization factor, the curves of Fig. 3 have been redrawn to give Fig. 6, where the ordinate is now in photons per Mev region per cm², per 100 roentgen.

In Fig. 7 the number of photons in any given Mev region is plotted as a function of the maximum energy

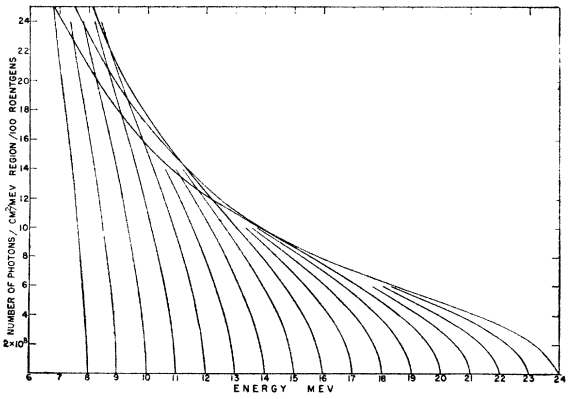

FIG. 6. Absolute photon distribution at the sample as a function of photon energy normalized to 100 "roentgens" (100 r) measured in lucite.

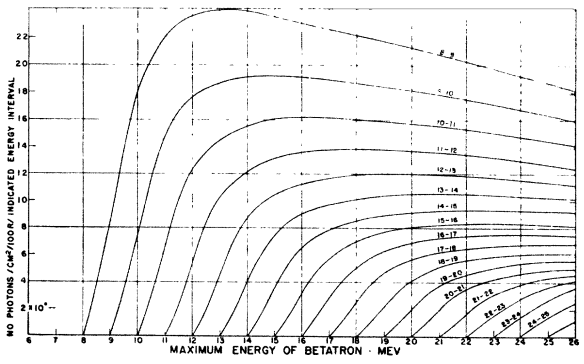

FIG. 7. Number of photons per cm² per indicated energy interval per 100 r measured in Lucite as a function of the maximum photon energy of the betatron.

of the betatron. For example, the number of photons between 8 and 9 Mev is given by the uppermost curve for different maximum energies of the betatron. The falling of this curve at higher energy is caused by normalization to the same dose. These curves are used directly to calculate the cross section.

Experimentally, several samples of the chosen element are irradiated at various maximum energies of the betatron. The number of product nuclei present at any time t_2 following the irradiation is given by

$$N=B/\lambda(1-e^{-\lambda t_1})\exp[-\lambda(t_2-t_1)], \quad (5)$$

where B is the rate of production of product nuclei in the sample, λ is the decay constant of the product nu-ured from the start of irradiation.

Using this formula, the observed activity may be normalized to saturation at an irradiation rate of 100 r/min. Figure 8 shows the normalized activity curves of Cu^{63}, Ta^{181}, and Sb^{121}.

The method by which the activity curves of Fig. 8 can be resolved into cross-section curves is illustrated in Fig. 9. Figure 9(a) shows an assumed cross-section curve, where σ_1 refers to the average cross section from 11 to 12 Mev, etc. Figure 9(b) is a sketch approximating Fig. 7, and Fig. 9(c) is a sketch representing Fig. 8. When the maximum energy of the betatron is 12 Mev, the activity $k=\sigma_1 a$. We can thus represent the activities k, l, m, etc., of Fig. 9(c) by the following set of equations:

$$\begin{aligned} k&=\sigma_1 a_1, \\ l&=\sigma_1 a_2+\sigma_2 b_1, \\ m&=\sigma_1 a_3+\sigma_2 b_2+\sigma_3 c_1, \text{ etc.} \end{aligned} \quad (6)$$

These linear equations can be solved for the unknowns, $\sigma_1, \cdots, \sigma_n$, yielding the desired cross-section curve.

The method is complicated by experimental error in $k, l, m, \cdots$ of the order of 2 percent. Because the computation involves the difference of two numbers of nearly the same magnitude, the error in some values of σ may be 50 percent. In general, because of the nature of the curves, if the calculated value of σ_j is too large, the value of σ_{j+1} will be too small by a greater percentage. This results in an oscillating, rather than a smooth, cross-section curve particularly if the uncertainty in the activity curve is large. However, approximate values can be calculated and progressive smoothing used to obtain a smooth curve. At higher energies the calculation of a negative cross section is an indication that some of the earliest estimated cross sections were too large.

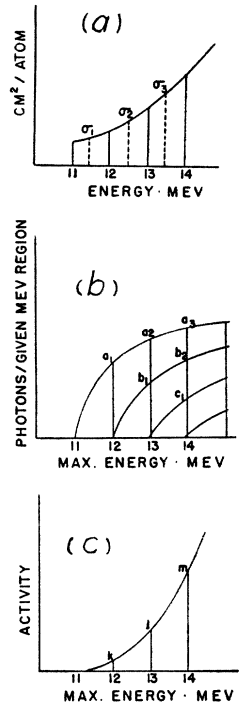

FIG. 9. (a) Sketch of a hypothetical cross section. (b) Sketch of Fig. 7. (c) Sketch of a saturated activity curve.

III. EXPERIMENTAL PROCEDURE

The dose given to a sample is recorded by the monitor (Fig. 2). The ionization current from the monitor charges a condenser to a predetermined value, at which

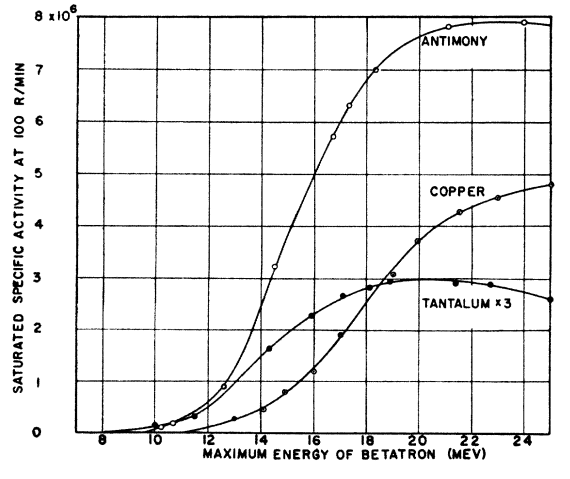

FIG. 8. Activity induced in 1 g of the isotopes Cu^{63}, Sb^{121}, and Ta^{181} if irradiated at 100 r.pm.. until saturation, after corrections have been applied for geometry, self-absorption, etc.

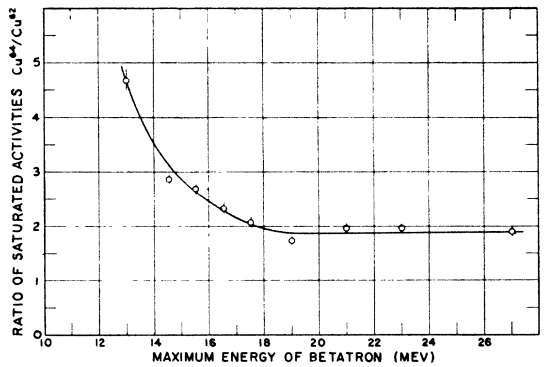

FIG. 10. Ratio of the saturated activity of Cu^{64} to that of Cu^{62} after a correction has been applied for the decay scheme of Cu^{64}.

point a counter and relay operate. The relay discharges the condenser, allowing the process to repeat. Each count or "click," therefore, represents a definite amount of radiation which has passed through the monitor. The number of "roentgens" per click can be determined in any sample position by placing the Victoreen r-meter at that point and taking several measurements.

Experimentally, after the monitor is calibrated with the Victoreen, a sample of cross-sectional area similar to the thimble chamber is placed in the holder and given a known dose in a measured time. After irradiation it is placed under an end-on counter and the activity measured. Separate experiments are performed to measure geometrical efficiency, self-absorption, and backscattering. The application of these corrections gives the absolute normalized activity curve shown in Fig. 8.

IV. RESULTS

A. Copper

Samples of 425 mg/cm^2 thickness and 1.1 by 2 cm size were irradiated between $\frac{1}{16}$-in. sheets of cadmium. The decay curve indicated 10.1 min. and 12.8 hour activities. The latter was negligible if the sample was counted within 20 minutes of the end of irradiation.

The Cu^{64} activity curve was found by measuring the ratio of the 12.8 hour to the 10.1 min. activities. Figure 10 shows the ratio of the saturated activities. Cu^{64} has a rather complex decay scheme,* some of the atoms going to Zn^{64} by β^- (36.5 percent) emission while others go to Ni^{64} by positron emission (17.5 percent) or K-capture (46 percent). The activity measured was corrected for the loss of counts due to K-capture by multiplying all measured counting rates by 1.85.

Figure 11 shows the absolute cross sections of Cu^{63} and Cu^{65}. The broken curve is due to McElhinney *et al.*[2] for Cu^{63}. A recent determination by Almy and Diven,[9] in excellent agreement with this work, is also shown. Wäffler and Hirzel[14] give $1.2\pm0.3\times10^{-25}$ cm^2 at 17.5 Mev. Our value of 1.1×10^{-25} is within their probable error.

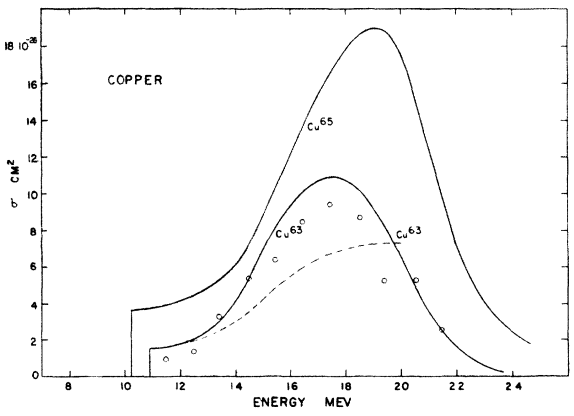

FIG. 11. Cross section for the (γ, n) reaction in Cu^{63} and Cu^{65}. The broken line is the results of McElhinney *et al.* (reference 2) for Cu^{63}. The plotted points are the results of B. C. Diven and G. M. Almy (to be published).

* To obtain the branching ratios, the data of H. Brandt et al. Helv. Phys. Acta **19**, 219 (1946) was combined with that of R. Bouchez and G. Kayes, J. de phys. et rad. (Ser. 8) **10**, 110 (1949).

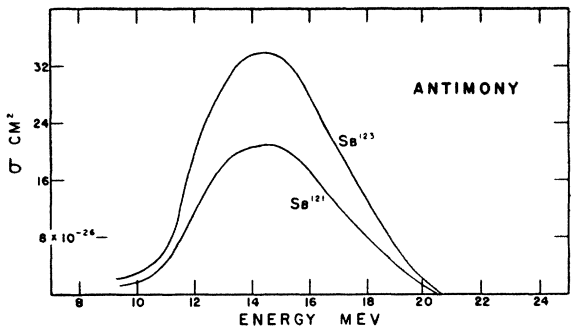

FIG. 12. Cross sections for the (γ, n) reaction in Sb^{123} and Sb^{121}. The cross section of Sb^{121} is only for those reactions which lead to the 16.4-min. isomeric state.

B. Antimony

Powdered antimony was irradiated in a cadmium thimble the same size as the Victoreen thimble chamber.

The decay showed 16.4±0.1-min. and 66-hour activities. When the longer activity is not subtracted, a 17.0-min. activity, which has previously been mentioned in the literature, is obtained. The authors believe the 16.4±0.1-min. half-life to be correct.

The Sb^{123} activity curve was determined independently, but found to be approximately 1.62 times the Sb^{121} after all corrections were applied.

Figure 8 shows the Sb^{121} activity curve and Fig. 12† the Sb^{121} and Sb^{123} cross-section curves.

C. Tantalum

Samples of 260 mg/cm^2 thickness and 1.1 cm by 2 cm size were irradiated and counted on thin plastic film. The decay curve showed a pure 8.0-hour activity.

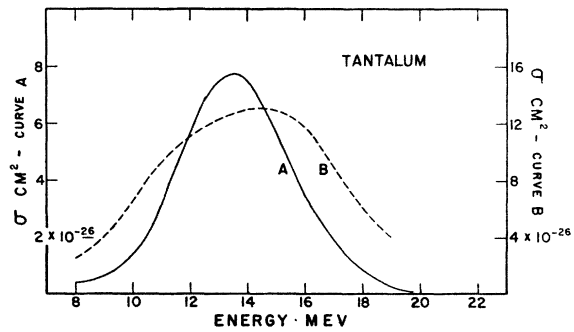

FIG. 13. Cross sections for the (γ, n) reaction in Ta^{181}. No correction has been made for K-cap ture. The broken curve is the results of McElhinney *et al.* (reference 2).

[14] H. Wäffler and O. Hirzel, Helv. Phys. Acta. **21** (Nos. 3–4), 200–3 (1948).

† The cross section given for $Sb^{121}(\gamma h)Sb^{120}$ is only for those reactions which lead to the 16.4-min. isomeric state. To obtain the total cross section for reactions going directly to the ground state of Sb^{120}.

TABLE II. Summary of the results of the cross-section measurements.

Parent isotope	Threshold Mev	Energy of maximum σ Mev	Maximum σ Barn	Half-width Mev	Integrated cross section Mev-Barn
Cu^{63}	10.9	17.5	0.11	6.0	0.70
Cu^{65}	10.2	19.0[a]	0.18	6.0	1.40
Sb^{121}	9.3	14.5	0.21	5.5	1.2
Sb^{123}	9.3	14.5	0.34	5.5	2.0
Ta^{181}	8.0	13.5	0.078	4.5	0.39

[a] The position of this maximum is not believed to be as accurately located as to the other substances.

Figure 8 shows the normalized activity curve and Fig. 13 the calculated cross section.‡ The result of McElhinney *et al.*[2] is indicated by the broken line.

V. DISCUSSION OF RESULTS

Table II shows the significant features of these cross-section measurements.

The most striking feature of the (γ, n) curves obtained in this work is their broadness. They give a "resonance width" of about 5.5 Mev, which is considerably broader than that found by Baldwin and Klaiber, though in good agreement with the measurements of McElhinney *et al.* and the more recent work of Almy and Diven. The cross-section *vs.* energy values obtained by these latter workers are plotted on top of our smooth curve in Fig. 11, the agreement being much better than one would expect from the estimated accuracy of the measurements.

Although the theory of Levinger and Bethe does not say anything about the expected "resonance width" in these reactions, it does predict the mean energy for photon absorption. According to their Eq. (40) and (42), this mean energy cannot be lower than 16 Mev. The values for this quantity are given in Table III and are seen to be less than 16 Mev in the case of antimony and tantalum. Competing reactions with relatively large integrated cross sections may raise these values considerably and bring them in closer agreement with theory. According to Levinger and Bethe, the integrated total cross section $\int \sigma dE$ should vary as NZ/A, or nearly as A, where σ is the total cross section for all reactions, $(\gamma, n)(\gamma, p)(\gamma, x)$, etc., at energy E. The values of this integral for the (γ, n) reactions only are listed in Table II and, as can be seen, are not linear in A. In order to retain the theory one would have to postulate a very large competing reaction in the case of tantalum or a large correction for K-capture.

TABLE III. Harmonic mean energies of the various reactions involved and a check on the validity of assuming that the photon distribution over the energy region giving rise to the activity varies as $1/E$. $\bar{E}$ is the mean energy for photon absorption.

Parent isotope	$\bar{E}$ Mev	E_H Mev	$\int \sigma(\gamma, n) dE/E$ Barn	$\frac{C_{24}}{P_m E_m}$ Barn
Cu^{63}	17.5	17.0	0.041	0.52
Sb^{121}	14.5	14.3	0.084	0.084
Sb^{123}	14.5	14.5	0.137	0.136
Ta^{181}	13.5	13.3	0.029	0.027

‡ No correction has been applied for undetected activity due to K-capture and internal conversion since the decay scheme of Ta^{180} is not known.

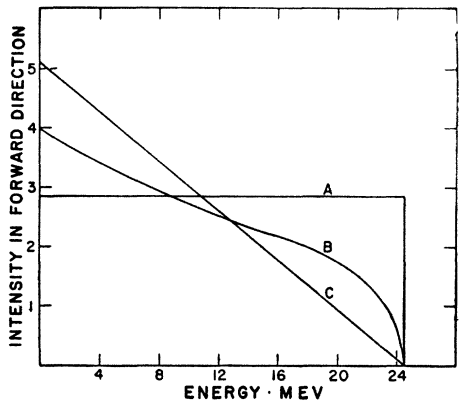

FIG. 14. Intensity in the forward direction for the assumed distributions: *A*. *A* $1/E$ photon distribution with a finite number of photons at the maximum energy. *B*. Schiff distribution. C. *A* $(E^{-1}-E_0^{-1})$ photon distribution with zero photons at the maximum energy.

If we assume that $P(E, E_0)$ gives the number of photons per cm² per Mev interval, then the number of active atoms produced in a given sample during an irradiation is

$$\int_0^{E_0} \sigma_{(\gamma, n)} P dE = C_{E_0}, \tag{7}$$

where E_0 is the maximum energy of the bremsstrahlung from the betatron. In our determination of cross section the systems of linear equations (6) express such sets of integrals with the integral being evaluated in each case by the trapezoidal rule. If $E_0 = 24$ Mev, then the area under the σP *vs.* E curve is actually made in our computation to be equal to the measured value of C_{24}.

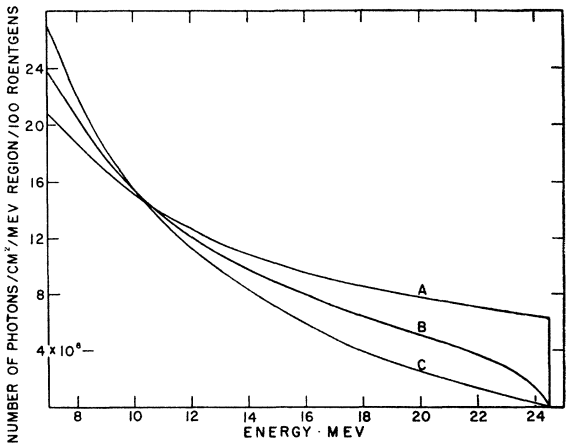

FIG. 15. Absolute photon distributions at the sample corresponding to the assumptions shown on Fig. 14. These have been normalized to 100 "roentgens" measured in Lucite.

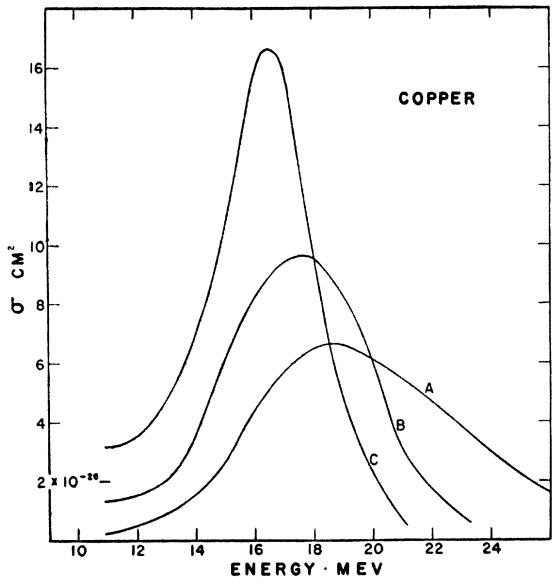

FIG. 16. Cross sections of copper which result from the three distributions of Fig. 14.

Assuming that the photon spectrum varies as $1/E$ we can write

$$P=P_mE_m/E, \tag{8}$$

where E_m is the energy at which $\sigma_{(\gamma,n)}$ has its maximum value and P_m is the value of P at this energy. Then to a fair approximation,

$$\int_0^{24}\sigma_{(\gamma,n)}dE/E=C_{24}/P_mE_m. \tag{9}$$

The actual values of the integral were determined by graphical integration and are listed in Table III. Their difference from C_{24}/P_mE_m values which are listed is an indication of the validity of Eq. (8). The disagreement is large in the case of copper because the peak of the cross-section curve is in this case too near the maximum energy of the spectrum, and, as can be seen from Fig. 6, the assumed equation does not give a good fit in this region.

The harmonic mean energy defined by Levinger and Bethe,

$$E_H=\left(\int\sigma_{(\gamma,n)}dE\right)\Big/\left(\int\sigma_{(\gamma,n)}dE/E\right),$$

is also listed in Table III.

The authors wish to express their appreciation for a grant from the N.R.C. and a bursary held by one of them (R.D.) which made this project possible. They also wish to thank L. Pease who measured the ratio of the Cu^{64}/Cu^{62} activity and S. B. Mauchel, betatron technician, for his untiring assistance.

APPENDIX

The dependence of the calculated cross-section shape upon the assumed photon distribution was investigated. Figure 14 shows the intensity in the forward direction for a maximum photon energy of 24.5 Mev for three assumed intensity distributions. Figure 15 shows the corresponding photon distributions normalized to give 100 "roentgens" as shown previously. These distributions are:

A. A $1/E$ photon distribution with a finite number of photons at the maximum energy.

B. Schiff distribution.

C. A $(E^{-1}-E_0^{-1})$ photon distribution with zero photons at the maximum energy.

Figure 16 shows the cross sections calculated using these assumed photon distributions.

Going from assumptions A to C it is seen that the maximum of the cross-section curve is shifted to lower energies, the half-width decreases and $\int\sigma_{(\gamma,n)}dE$ decreases. This indicates, however, that the cross section is only moderately sensitive to the assumed distribution, since relatively large variations in it do not produce correspondingly large variations in the cross-section shape and especially in $\int\sigma_{(\gamma,n)}dE$. Therefore, we would not expect smaller corrections to the Schiff formula to affect our results appreciably.

The resolving power of this method was also investigated. It was found that it would not resolve two rectangular cross sections 1 Mev in width and separated by 2 Mev. Thus, these results give only the general features of the cross section and do not indicate what the finer structure, if any, may be.